THE JOURNAL OF PHYSICAL CHEMISTRY C

Article

pubs.acs.org/JPCC

Spectroscopic Evidence of Work Function Alterations Due to Photoswitchable Monolayers on Gold Surfaces

Matthew A. Bartucci, Jan Florián, and Jacob W. Ciszek*

Department of Chemistry and Biochemistry, Loyola University Chicago, 1032 West Sheridan Road, Chicago, Illinois 60660, United States

Supporting Information

ABSTRACT: Taking advantage of surfaces' response to interfacial dipoles, a class of photochromophores (dihydroindolizine) is demonstrated to alter the work function of the underlying substrate (~170 meV). This same molecule also provides spectroscopic signatures for correlating the change in molecular structure to the induced change in the surfaces' electronic properties. Polarization modulation infrared reflection absorption spectroscopy (PM-IRRAS) allows analysis of the characteristic dihydroindolizine C=C (1559 cm^{-1}) and pyridinium (1643 cm^{-1}) stretch as a function of photoexcitation. Structural assignments of this photochromophore are corroborated to density function theory calculations. Conformational changes in the monolayers appear in parallel with work function changes and are consistent with both its rate and magnitude.

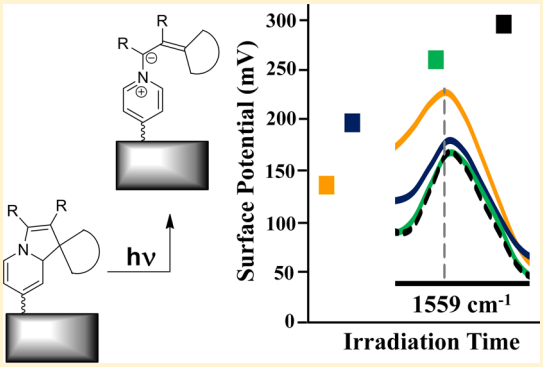

INTRODUCTION

Work function (i.e., Fermi level) modulation of metal electrodes, due to an adsorbed organic monolayer, allows modern electronic devices such as organic light emitting diodes and organic field effect transistors to operate in a more efficient manner.[1−6] The majority of devices are inherently hindered by a high contact resistance that is caused by the misalignment of the Fermi energy of the metal and the highest occupied molecular orbital (HOMO) or lowest unoccupied molecular orbital (LUMO) of the bulk organic.[6−8] To minimize misalignment, the metal's Fermi level can be altered via self-assembled monolayers (SAMs).[9−11] The molecular and interfacial dipoles of the adsorbed SAMs "tune" the Fermi level of the metal with respect to either the HOMO or LUMO of the organic channel, allowing for improved hole or electron transport.[12−14] For example, either straight chain hydrocarbons or fluorinated alkanes can respectively decrease[10,15] or increase[10,16] the work function of the substrate with a high degree of correlation to the aforementioned dipoles (Figure 1a).[13]

Recently, photoreversible work function alterations based on a trans−cis conformation change of azobenzene monolayers have been observed.[17−19] Here, incident light induces the isomerization, which alters the dipole of the monolayer and, in turn, generates a measurable shift in the work function of the underlying metal. If such work could be extended to a second class of photochromophores (dihydroindolizines, DHIs), which has both obvious spectroscopic signatures and large persistent dipoles (~3−5 D), a simple correlation between molecular change and substrate perturbation could be reached.

In this paper, surface infrared signatures of DHI molecules are used in conjunction with Kelvin probe measurements of the surface potential to demonstrate light-induced changes to the molecular monolayer and the resulting change in the substrate's work function (Figure 1b). DFT calculations of vibrational states allow for nuanced discussion of the molecular change, the resulting molecular dipole, and its effect on the surface's work function.

METHODS

Experimental Methods. Ethanol (200 proof), 3,3,4,4,5,5,6,6,7,7,8,8,9,9,10,10,10-heptadecafluoro-1-decanethiol (FDT), 1-dodecanethiol, and 1-octadecanethiol (ODT) were purchased from Sigma-Aldrich and used without additional purification. The syntheses of **DHI-5** and **-6** (Figure 1b) are reported in the Supporting Information (Scheme S1). The DHIs were kept in the dark at all times (excluding photoisomerization studies).

Metal evaporations were performed in a Kurt J. Lesker NANO 38 thermal evaporator. The thicknesses of monolayers on gold were determined with a Gaertner stokes ellipsometer LSE. Solution and solid-state UV−vis spectra were acquired on a Shimadzu UV-2550 spectrometer. IR spectra of solid-state KBr samples were obtained with a Tensor 37 FT-IR from Bruker Optics with MCT detector. Surface IR spectra were acquired on a Tensor 37 FT-IR from Bruker Optics with polarization modulation accessory (PMA 50) and MCT

Received: June 10, 2013
Revised: August 19, 2013
Published: August 21, 2013

   dx.doi.org/10.1021/jp405710u | J. Phys. Chem. C 2013, 117, 19471−19476

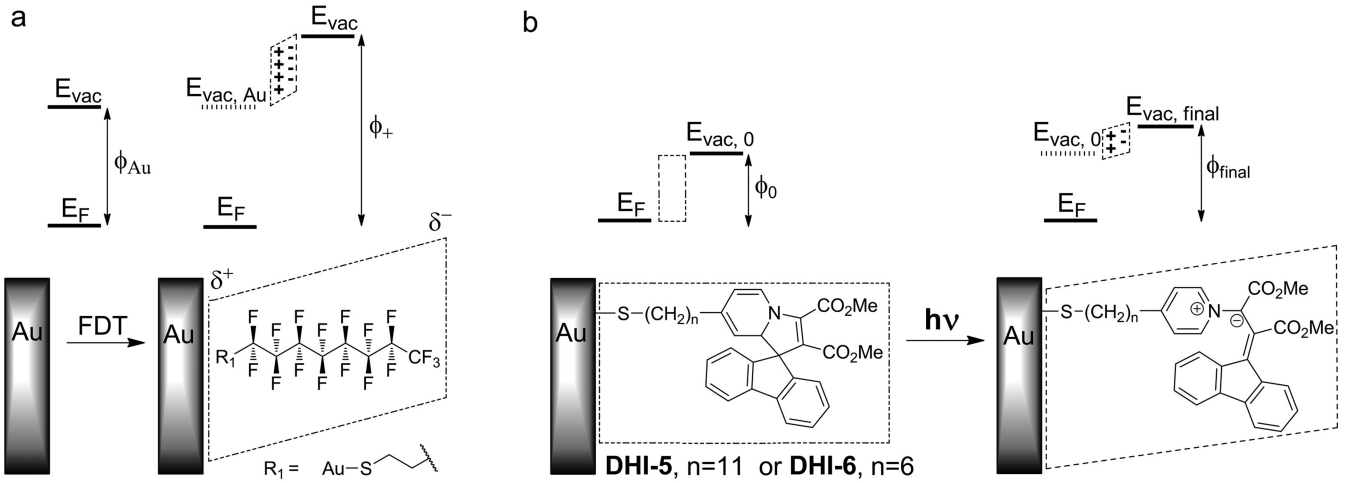

Figure 1. (a) Energy diagram of bare gold and gold that has been modified with 3,3,4,4,5,5,6,6,7,7,8,8,9,9,10,10,10-heptadecafluoro-1-decanethiol (FDT). The molecular dipole orientation of the FDT monolayer increases the work function with respect to bare gold. (b) The spiro DHI adsorbed onto gold. In this state, the molecule has a small, nonzero, dipole perpendicular to the surface and a corresponding initial work function that is similar to a straight chain alkane. (right) Zwitterionic DHI after being excited with 400 nm light, which affords a dipole oriented similarly to the FDT monolayer. This results in an increase in the work function when compared with the spiro species. Dashed boxes in the energy diagram represent the dipole of the monolayer.

detector. DHI irradiations utilized a 400 or 501 nm LED (12 mW/cm^2), and all surface potential data were obtained via a Kelvin probe from KP Technologies. With the exception of ellipsometry and UV–vis, all measurements were made under nitrogen.

Assembly substrates were prepared as follows: Glass slides were cleaned in a piranha solution (3:1 H_2SO_4/H_2O_2) for 30 min at ~100 °C and washed copiously with 18 MΩ water. The glass samples were dried extensively with nitrogen before being placed in the thermal evaporator. Gold (125 nm) was thermally evaporated onto the freshly cleaned slides with a 5 nm chromium adhesion layer at a base pressure of $<1 \times 10^{-6}$ Torr and a deposition rate of 1 Å/s.

The disulfide functionality of **DHI-5** and **-6** allows for facile self-assembly of organized monolayers onto gold surfaces from solution.[20,21] Both thiol (FDT, ODT, dodecanethiol) and disulfide assemblies were performed in high-purity ethanol that was degassed for 30 min with nitrogen prior to use. Assembly concentrations ranged from 0.1 to 0.5 mM, and times were 14–20 h. After assembly, samples were rinsed with ethanol and dried with nitrogen. For the DHIs, all assembly procedures were performed in the dark. During assembly solution preparation, the DHIs were sonicated to mediate dissolution. After assembly, the substrates containing the DHI monolayer were placed in fresh ethanol, sonicated to remove excess DHI, before drying with nitrogen. Ellipsometry was used to confirm monolayer coverage. Measured thicknesses match the corresponding theoretical values[22] to within ±2 Å.

All Kelvin probe measurements of surface potential were referenced to an ODT monolayer ($\Delta\Phi = \Phi_{SAM} - \Phi_{ODT}$). ODT-gold serves as a consistent, reproducible reference, and its work function is reported to be 1.2 eV smaller than bare gold (3.9 eV for ODT-gold and 5.1 eV for bare gold).[16,23]

Theoretical Methods. Quantum-mechanical calculations of the structure and vibrational spectra of the spiro and zwitterionic forms of DHI were carried out using the B3LYP/6-31G* hybrid density functional theory (DFT) method implemented in the Gaussian 03 program.[24] In these calculations, the alkane chain (Figure 1b) was replaced by a hydrogen atom. IR spectra of the spiro and zwitterionic forms of DHI were modeled as the Boltzmann-weighted average of the spectra of the two lowest-energy conformers of each form. The calculated frequencies were scaled by a factor of 0.96 that was determined by comparing B3LYP/6-31G* and experimental frequencies of CN, CC, and CO stretching vibrational modes of cytosine.[25]

RESULTS AND DISCUSSION

Characterization of the Photoswitch via UV–Vis and IR Spectroscopies. DHIs, as a class, exist in two forms: the stable spiro form and the zwitterion form, which can be accessed via photoisomerization (Figure 1b). This transition is characterized by the molecules' optical absorptions, particularly the π to π^* transition (360–410 nm) in the spiro species and a presumed charge transfer transition (500–700 nm) for the photoisomerized, zwitterionic, species.[26]

This DHI subunit (terminal end, Figure 1b) has been incorporated into two molecules, **DHI-5** and **-6**. The second half of the molecule, the aliphatic chain which links the DHI to the surface, is variable, and was chosen for these studies because of simpler vibrational interpretation of switched states, in contrast to conjugated systems.[27] Furthermore, the extended alkyl system limits energy and electron transfer to surfaces that can complicate the photochemistry.[28]

Both **DHI-5** (Figure 2a) and **-6** (Supporting Information, Figure S1a) undergo the same optical transitions. In the spiro state, the π-to-π^* transition for **DHI-5** (386 nm) occurs well within the accepted range of established DHIs. When irradiated with 400 nm light, the presumed charge transfer band appears at 583 nm (Figure 2a), confirming the generation of the stable, persistent zwitterion. Transitions differ by only ±3 nm for **DHI-6**. These measurements, performed in the solid state, mirror solution data (Figure S2, Supporting Information).

As the optical properties change, accompanying vibrational differences are expected. Specifically, the stretches of double bonds in the dihydropyridine ring should diminish, whereas the frequencies corresponding to the pyridinium ion are expected to appear (Figure 2a, inset). It should be noted that the DHI

dx.doi.org/10.1021/jp405710u | J. Phys. Chem. C 2013, 117, 19471–19476

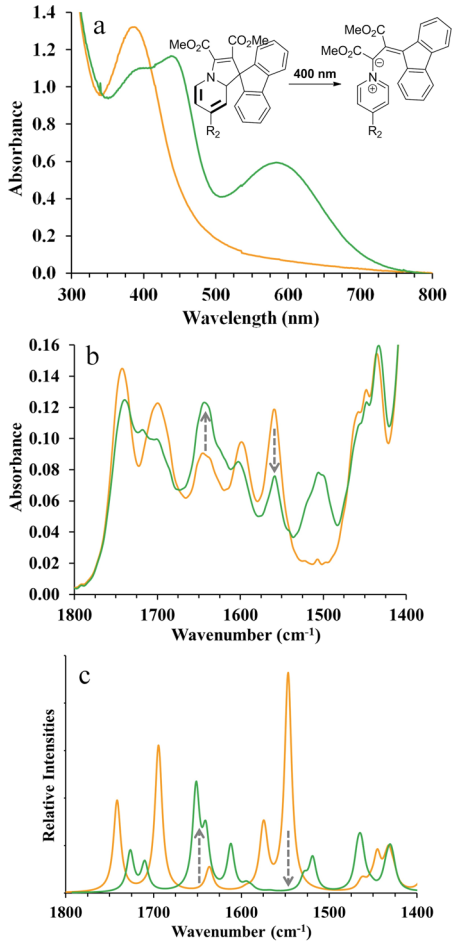

Figure 2. Solid-state (KBr) correlation study of (a) UV−vis and (b) IR of **DHI-5**. Yellow curves represent spiro DHI. The sample was irradiated for 1.5 min generating a persistent zwitterion conformer (green curves) in the solid state. Additional irradiation yielded no further change in either spectra. The gray dashed arrows show an increase in the zwitterion character at 1643 cm^{-1} along with a decrease of the isolated olefins signal at 1559 cm^{-1}. Spectra shown in panels a and b correspond to the same sample run consecutively. (c) Calculated DFT vibrational spectra displays a new increase for the zwitterion at 1651 cm^{-1} and the disappearance of the stretch at 1547 cm^{-1}, which are represented by the dashed arrows. Changes are consistent with the experimental solid-state switch.

moiety in the zwitterionic form could potentially exist in different conformers;[26,29,30] however, the formation of the aromatic pyridinium ion is consistent with all variations of the zwitterion and is an obvious spectroscopic signature for the IR data. Such signals are apparent in our experimental spectra (Figure 2b) and can be explained as follows:

For the spiro conformer, the characteristic vibrations of the C═C bonds in the dihydropyridine ring are typically observed near 1650 and 1580 cm^{-1} and appear at 1645 and 1559 cm^{-1} in **DHI-5**.[31−33] In the scaled B3LYP/6-31G* vibrational spectrum (Figure 2c), the corresponding normal modes lie at 1638 and 1547 cm^{-1}, and the assignment can be confirmed (Supporting Information Figures S3−11 show atomic displacement vectors during normal vibrations for the major peaks). In this instance, the calculations also show the 1547 cm^{-1} mode to contain significant contribution from the stretching vibration of the C═C bridge between the two ester groups. Readers curious about interpretation of other modes can find them in Supporting Information Table S1.

When this sample is irradiated to promote formation of the zwitterion, the IR spectrum shows new stretches for the pyridinium ion in conjunction with the appearance of the charge transfer transition band in the visible spectrum. The two normal vibrations that are correlated to this appearance are observed near 1643 and 1506 cm^{-1}. IR bands in these regions are commonly assigned to the stretching vibrations of the pyridinium ring.[34,35] Our calculations show that each of these two bands corresponds to the stretching vibrations of the pyridinium ring that are coupled to the C═O stretch of one of the two ester groups (Supporting Information Table S1). The appearance of the two bands at each location of the calculated spectrum (and shoulders in the experimental) is due to presence of two rotational conformers of the zwitterionic DHI. The contribution of the stretch of the polar C═O bond to these normal modes explains the large IR intensity increase in this spectral region upon DHI irradiation by the UV light (Figures 2b, c). Both vibrations can be used diagnostically to discern the state of the DHI but, for reasons discussed later, we focus on the peak at 1643 cm^{-1}.

In addition to the intensity increase at 1643 cm^{-1}, the spiro/zwitterion switch can be monitored via the decrease in the IR intensity of the dihydropyridine C═C bonds at 1559 cm^{-1}. This spectral change is consistent with our calculations that show a strong IR band at 1547 cm^{-1} for the spiro DHI but no band for the zwitterionic DHI in this spectral region (Figure 2c). As such, this spiro C═C stretch can be used to provide a semiquantitative measure of the percentage of photochromophores that have switched. Implicit here is the fact that only about one-third of photochromophores are in the zwitterionic form in the solid state (Figure 2b), even if irradiation is extended. This hypothesis is consistent with the presence of the shoulder in the UV−vis data (~390 nm). Both the peaks at 1643 and 1559 cm^{-1} will provide a spectroscopic handle for subsequent identification of the molecular DHI on the surface for Kelvin probe measurements.

Photochemically Induced Work Function Shifts and Correlation with Spectroscopic Signatures. To test the photochromophores' ability to dynamically tune a metal's work function, both **DHI-5** and **-6** were assembled onto freshly prepared gold and were compared with freshly prepared ODT monolayers via a Kelvin probe, which measures the surface potential difference between substrates. For these measurements, the standard deviation from the mean for the measurement at a single point was quite low: 5 mV. The deviation across multiple samples was higher; the average spiro surface potential for **DHI-5** and **-6** were found to be at 28 ± 42 and 148 ± 84 mV, respectively, relative to ODT on gold. The higher standard deviation for the spiro **DHI-6** is presumably related to less efficient packing and higher disorder often reported for shorter alkyl chains.[22] Surface spectroscopy for both spiro DHIs correlates well with the solid-state data (vide infra), providing evidence for the integrity of the assembled material.

When spiro **DHI-5** and **-6** were irradiated for 13 min with 400 nm light, the surface potential increased by 178 and 164 mV from their respective initial values (Figure 3, circles and squares). These individual samples, which were correlated with their spectroscopy, are representative of a greater trend: on average, the shift for five **DHI-5** samples at 13 min irradiation was 186 mV with a standard deviation of 23 mV. The direction

dx.doi.org/10.1021/jp405710u | J. Phys. Chem. C 2013, 117, 19471−19476

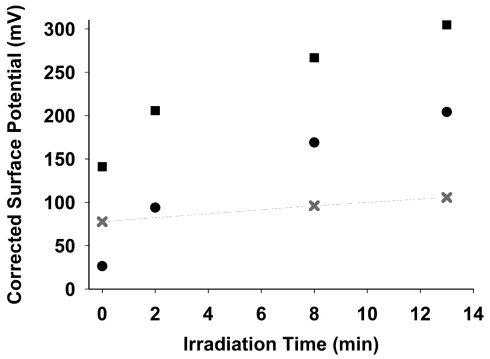

Figure 3. Kelvin probe measurements of **DHI-5** (●) and **DHI-6** (■). The DHIs were irradiated with 400 nm light for 0, 2, 8, and 13 min, and an active shift in the surface potential was noted, corresponding to the zwitterion species. When **DHI-6** was irradiated with 501 nm light (×), a negligible shift was observed.

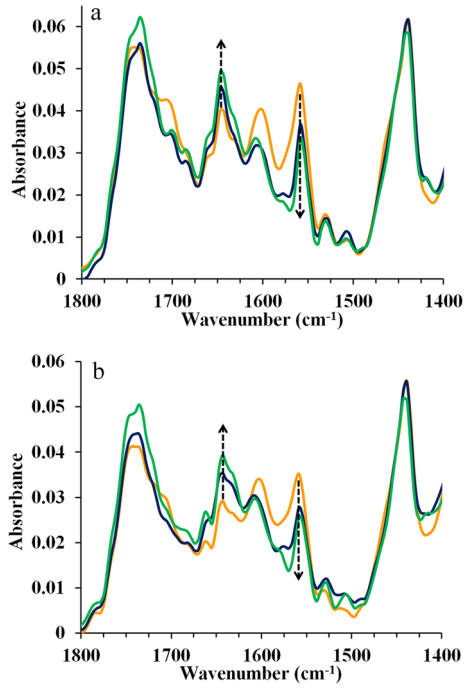

Figure 4. PM-IRRAS of spiro (yellow) monolayers of (a) **DHI-5** (b) **DHI-6**. Irradiation times of 2 (blue), and 8 (green) minutes support the formation of the zwitterion on the surface. Dashed arrows represent formation of the pyridinium ring (1644 cm^{-1}) and the decrease in the isolated olefins (1559 cm^{-1}).

of the work function shift from this data is consistent with the orientation of the molecular dipole of the zwitterion with respect to the surface, suggesting that we are observing the effect of DHI switching from its spiro to zwitterionic form. The molecular origin of this effect can be supported by two additional observations. First, no/minimal absorption, and thus, isomerization, is expected for 501 nm light (Figure 2a). As expected, DHI monolayers irradiated with this wavelength show an insignificant change (Figure 3). Second, a sample of 1-dodecanethiol assembled on gold was irradiated with 400 nm light, and the measured shift from irradiation was negligible (21 mV), allowing us to rule out other effects, such as photo-oxidation of the Au−S bond. This second data set can be found in the Supporting Information (Figure S12). Combined, the results show that it is possible to dynamically shift the work function of a material, based on molecular effects, by ∼170 meV.

The same DHI samples reported in Figure 3 were examined sequentially via polarization modulation infrared reflection absorption spectroscopy (PM-IRRAS) so that the electronic switch could be correlated with the vibrational signatures of the zwitterion. For the first two irradiation intervals (0−2 and 2−8 min), the same increase (∼70 mV) was observed for each measurement. The substantial shift appears in conjunction with vibrational evidence for isomerization, with an increase in (1644 cm^{-1}) pyridinium bond character and the decrease in the isolated dihydropyridine C═C bond (1559 cm^{-1}) (Figure 4). For the final 5 min of irradiation (8−13 min), a smaller increase of 35 mV was observed, and as expected, the differences in spectra are less pronounced, suggesting minimal change in configuration. In fact, the **DHI-6** sample shows virtually no vibrational changes, whereas **DHI-5** shows minor changes at 1559 cm^{-1}. These have been omitted for clarity but can be seen in the Supporting Information (Figure S13). The electronic and spectroscopic changes were consistent for all DHI samples that were subjected to the same experiment. This IR/Kelvin probe analysis was simplified by the fact that the switch has an extraordinarily slow relaxation time on the surface (a minimally relaxed 90 h spectrum can be seen in Supporting Information Figure S14), and thus, the time required for data acquisition has little effect on the system.

In examining this data, a brief comment on the region at ∼1500 cm^{-1} is warranted. In the initial characterization of the photoswitch (as a KBr pellet, Figure 2b), three absorptions appear to be highly correlated with the change from the spiro form to zwitterion; only two are observed for the monolayer samples (1644, 1559 cm^{-1}). The stretch at 1506 cm^{-1}, which according to DFT calculations corresponds to the C═C bond formed at the 9-position of the fluorene moiety (Figure 2), does not appear in the surface IR of the irradiated samples (Figure 4; 2, 8 min). A common explanation for these situations is the surface selection rule. The net dipole of the vibrations that are parallel to the surface are nullified by those from an image charge, and no absorption appears.[36] Naively, on the basis of the SAM tilt angles as well as molecular geometry (Figure 1b), one might expect this to be a case for the C═C bond at 1506 cm^{-1}. To confirm this hypothesis, DHIs were spin-coated onto the surface rather than assembled, and nonoriented multilayers of varying thicknesses were formed as a result. The randomly oriented multilayers display the missing stretch (Figure S15, Supporting Information). As the layer thickness decreases (and a greater portion of the signal is from molecules bonded to the surface), this peak decreases in intensity relative to the other signals.

Substituent Effects. **DHI-5** and **-6** serve as effective model systems for this class of photochromophores. However, as we begin to analyze the relationship between DHIs and the work function change, it would be ideal if the dihydropyridine C═C bond stretch were to remain diagnostic for other molecules within this subclass. If true, substituents impacting optical absorption, stability, the dipole, and even molecular orientation could be appended to the molecule.[26] Such flexibility would be extremely powerful for reconciling theoretical changes in the work function with experiment.

Preliminary analysis indicates this to be true. The indicative C═C stretch is present in other DHIs we have synthesized, where the alkyl chain has been exchanged for various alkynyl,

dx.doi.org/10.1021/jp405710u | J. Phys. Chem. C 2013, 117, 19471−19476

aryl, or oxy substituents. Stretches for the four compounds are reported at 1569, 1559, 1551, and 1547 cm^{-1}.[27] Of these, an alkynyl-substituted DHI (Figure 5) was examined both pre- and postirradiation for vibrational changes. The C═C peak at 1547 cm^{-1} is highly correlated with the switching event.

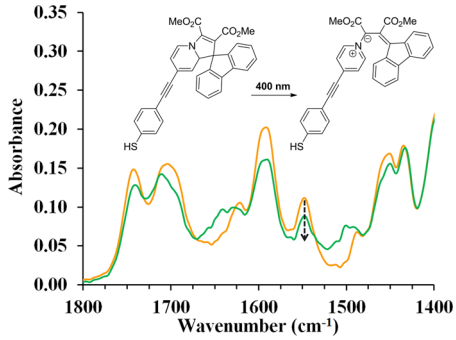

Figure 5. Solid-state (KBr) IR of alkynyl DHI. Yellow curves represent spiro DHI. Sample was irradiated for 15 min, generating a persistent zwitterion conformer (green curves) in the solid state. Additional irradiation yielded no further change. The black dashed arrow shows a decrease in the isolated olefins signal at 1547 cm^{-1}.

The above sequence of substitutions should allow for varying degrees of electron/energy transfer between the photochromophore and the surface, which inhibits switching.[28] Combined work function/spectroscopic analysis can clarify some of these effects. As such, the results reported in this work are fundamental to ongoing studies on work functions in the area.

CONCLUSION

An active shift in the work function of a gold surface was generated by two photochromic DHI monolayers. Surface IR suggests that the electronic alterations are caused by the light-induced change from the spiro to the zwitterionic species. Changes in the surface spectroscopy were confirmed via experimental solid-state spectroscopy and DFT vibrational calculations. Characteristic vibrational features appear general across the class of molecules and can be used for analysis of dihydroindolizines designed with other work function applications in mind.

ASSOCIATED CONTENT

Supporting Information

Synthesis of DHIs, associated characterization data (NMR, IR, MS) DFT normal mode assignments and atom displacement plots, and vibrational correlation study for **DHI-6**, solution UV−vis and corresponding half-life data, additional controls for the work function data, and thin film irradiation study of **DHI-6** are given. This information is available free of charge via the Internet at http://pubs.acs.org.

AUTHOR INFORMATION

Corresponding Author

*Phone: (773) 508-3107. Email: jciszek@luc.edu.

Notes

The authors declare no competing financial interest.

ACKNOWLEDGMENTS

This work was supported in part by a grant from the National Science Foundation (NSF), Career Award No. 1056400.

REFERENCES

(1) Yu, G.; Zhang, C.; Heeger, A. J. Dual-Function Semiconducting Polymer Devices: Light-Emitting and Photodetecting Diodes. *Appl. Phys. Lett.* **1994**, *64*, 1540−1542.
(2) Tang, C. W.; VanSlyke, S. A. Organic Electroluminescent Diodes. *Appl. Phys. Lett.* **1987**, *51*, 913−915.
(3) Burroughes, J. H.; Bradley, D. C.; Brown, A. R.; Marks, R. N.; Mackay, K.; Friend, R. H.; Burns, P. L.; Holmes, A. B. Light-Emitting Diodes Based on Conjugated Polymers. *Nature* **1990**, *347*, 539−541.
(4) Risko, C.; Zangmeister, C. D.; Yao, Y.; Marks, T. J.; Tour, J. M.; Ratner, M. A.; van Zee, R. D. Experimental and Theoretical Identification of Valence Energy Levels and Interface Dipole Trends for a Family of (Oligo)Phenylene-ethynylenethiols Adsorbed on Gold. *J. Phys. Chem. C* **2008**, *112*, 13215−13225.
(5) Ulman, A. Formation and Structure of Self-Assembled Monolayers. *Chem. Rev.* **1996**, *96*, 1533−1554.
(6) Ratner, M. Molecular Electronics: Pushing Electrons Around. *Nature* **2000**, *404*, 137−138.
(7) Hamadani, B. H.; Corley, D. A.; Ciszek, J. W.; Tour, J. M.; Natelson, D. Controlling Charge Injection in Organic Field-Effect Transistors Using Self-Assembled Monolayers. *Nano Lett.* **2006**, *6*, 1303−1306.
(8) Howell, S.; Kuila, D.; Kasibhatla, B.; Kubiak, C. P.; Janes, D.; Reifenberger, R. Molecular Electrostatics of Conjugated Self-Assembled Monolayers on Au(111) Using Electrostatic Force Microscopy. *Langmuir* **2002**, *18*, 5120−5125.
(9) Campbell, I. H.; Kress, J. D.; Martin, R. L.; Smith, D. L.; Barashkov, N. N.; Ferraris, J. P. Controlling Charge Injection in Organic Electronic Devices Using Self-Assembled Monolayers. *Appl. Phys. Lett.* **1997**, *71*, 3528−3530.
(10) Campbell, I. H.; Rubin, S.; Zawodzinski, T. A.; Kress, J. D.; Martin, R. L.; Smith, D. L.; Barashkov, N. N.; Ferraris, J. P. Controlling Schottky Energy Barriers in Organic Electronic Devices Using Self-Assembled Monolayers. *Phys. Rev. B* **1996**, *54*, 14321−14324.
(11) Evans, S. D.; Ulman, A. Surface Potential Studies of Alkylthiol Monolayers Adsorbed on Gold. *Chem. Phys. Lett.* **1990**, *170*, 462−466.
(12) de Boer, B.; Hadipour, A.; Mandoc, M. M.; van Woudenbergh, T.; Blom, P. W. M. Tuning of Metal Work Functions with Self-Assembled Monolayers. *Adv. Mater.* **2005**, *17*, 621−625.
(13) Ishii, H.; Sugiyama, K.; Ito, E.; Seki, K. Energy Level Alignment and Interfacial Electronic Structures at Organic/Metal and Organic/Organic Interfaces. *Adv. Mater.* **1999**, *11*, 605−625.
(14) Kelley, T. W.; Baude, P. F.; Gerlach, C.; Ender, D. E.; Muyres, D.; Hasse, M. A.; Vogel, D. E.; Theiss, S. D. Recent Progress in Organic Electronics: Materials, Devices, and Processes. *Chem. Mater.* **2004**, *16*, 4413−4422.
(15) Zehner, R. W.; Parsons, B. F.; Hsung, R. P.; Sita, L. R. Tuning the Work Function of Gold with Self-Assembled Monolayers Derived from X−$[C_6H_4$−C≡C−$]_n C_6H_4$−SH (n = 0, 1, 2; X = H, F, CH_3, CF_3, and OCH_3). *Langmuir* **1999**, *15*, 1121−1127.
(16) Alloway, D. M.; Hofmann, M.; Smith, D. L.; Gruhn, N. E.; Graham, A. L.; Colorado, R., Jr.; Wysocki, V. H.; Lee, T. R.; Lee, P. A.; Armstrong, N. R. Interface Dipoles Arising from Self-Assembled Monolayers on Gold: UV-Photoemission Studies of Alkanethiols and Partially Fluorinated Alkanethiols. *J. Phys. Chem. B* **2003**, *107*, 11690−11699.
(17) Suda, M.; Kameyama, N.; Ikegami, A.; Einaga, Y. Reversible Phototuning of the Large Anisotropic Magnetization at the Interface between a Self-Assembled Photochromic Monolayer and Gold. *J. Am. Chem. Soc.* **2009**, *131*, 865−870.
(18) Ah Qune, L. F. N.; Akiyama, H.; Nagahiro, T.; Tamada, K.; Wee, A. T. S. Reversible Work Function Changes Induced by Photoisomerization of Asymmetric Azobenzene Dithiol Self-Assembled Monolayers on Gold. *Appl. Phys. Lett.* **2008**, *93*, 083109.

(19) Nagahiro, T.; Akiyama, H.; Hara, M.; Tamada, K. Photoisomerization of Azobenzene Containing Self-Assembled Monolayers Investigated by Kelvin Probe Work Function Measurements. *J. Electron Spectrosc. Relat. Phenom.* **2009**, *172*, 128−133.
(20) Nuzzo, R. G.; Allara, D. L. Adsorption of Bifunctional Organic Disulfides on Gold Surfaces. *J. Am. Chem. Soc.* **1983**, *105*, 4481−4483.
(21) Love, J. C.; Estroff, L. A.; Kriebel, J. K.; Nuzzo, R. G.; Whitesides, G. M. Self-Assembled Monolayers of Thiolates on Metals as a Form of Nanotechnology. *Chem. Rev.* **2005**, *105*, 1103−1169.
(22) Porter, M. D.; Bright, T. B.; Allara, D. L.; Chidsey, C. E. D. Spontaneously Organized Molecular Assemblies. 4. Structural Characterization of *n*-Alkyl Thiol Monolayers on Gold by Optical Ellipsometry, Infrared Spectroscopy, and Electrochemistry. *J. Am. Chem. Soc.* **1987**, *109*, 3559−3568.
(23) Ge, Y.; Whitten, J. E. Interfacial Electronic Properties of Thiophene and Sexithiophene Adsorbed on a Fluorinated Alkanethiol Monolayer. *J. Phys. Chem. C* **2008**, *112*, 1174−1182.
(24) Frisch, M. J.; Trucks, G. W.; Schlegel, H. B.; Scuseria, G. E.; Robb, M. A.; Cheeseman, J. R.; Montgomery, J., J. A.; Vreven, T.; Kudin, K. N.; Burant, J. C., et al. In *Gaussian 03, revision C.02*; Gaussian, Inc.: Wallingford, CT, 2004.
(25) Florián, J.; Baumruk, V.; Leszczynski, J. IR and Raman Spectra, Tautomeric Stabilities, and Scaled Quantum Mechanical Force Fields of Protonated Cytosine. *J. Phys. Chem.* **1996**, *100*, 5578−5589.
(26) Durr, H.; Bouas-Laurent, H. *Photochromism: Molecules and Systems*; Elsevier: Amsterdam, 1990.
(27) Bartucci, M. A.; Wierzbicki, P. M.; Gwengo, C.; Shajan, S.; Hussain, S. H.; Ciszek, J. W. Synthesis of Dihydroindolizines for Potential Photoinduced Work Function Alteration. *Tetrahedron Lett.* **2010**, *51*, 6839−6842.
(28) Comstock, M. J.; Levy, N.; Kirakosian, A.; Cho, J.; Lauterwasser, F.; Harvey, J. H.; Strubbe, D. A.; Fréchet, J. M. J.; Trauner, D.; Louie, S. G.; et al. Reversible Photomechanical Switching of Individual Engineered Molecules at a Metallic Surface. *Phys. Rev. Lett.* **2007**, *99*, 038301.
(29) Shrestha, T. B.; Melin, J.; Liu, Y.; Dolgounitcheva, O.; Zakrzewski, V. G.; Pokhrel, M. R.; Goritchiani, E.; Ortiz, J. V.; Turro, C.; Bossman, S. H. New Insights in the Photochromic Spiro-Dihydroindolizine/Betaine-System. *Photochem. Photobiol. Sci.* **2008**, *7*, 1449−1456.
(30) Bleisinger, H.; Scheidhauer, P.; Durr, H.; Wintgens, V.; Valat, P.; Kossanyi, J. Photophysical Properties of Biphotochromic Dihydroindolizines. Ring-Opening into Extended bis-Betaines. *J. Org. Chem.* **1998**, *63*, 990−1000.
(31) Fry, E. M. 6-Cyano-1,2,5,6-tetrahydropyridines in the Preparation of 1,2-Dihydropyridines. Tautomerism of the Dienes. *J. Org. Chem.* **1964**, *29*, 1647−1650.
(32) Noland, W. E.; Lee, C. K. 2-Addition of Pyrroles to Dimethyl Acetylenedicarboxylate: Michael-Type Adducts and Diels−Alder Products. *J. Org. Chem.* **1980**, *45*, 4573−4582.
(33) Thiessen, L. M.; Lepoivre, J. A.; Alderweireldt, F. C. Preparation of 1,2,4-Trialkyl or Aryl Substituted 1,2-Dihydropyridines by Grignard Reagents. *Tetrahedron Lett.* **1974**, *1*, 59−62.
(34) Bae, I. T.; Huang, H.; Yeager, E. B.; Scherson, D. A. In Situ Infrared Spectroscopic Studies of Redox Active Self-Assembled Monolayers on Gold Electrode Surfaces. *Langmuir* **1991**, *7*, 1558−1562.
(35) Hester, R. E.; Suzuki, S. Vibrational Analysis of Methylviologen. *J. Phys. Chem.* **1982**, *86*, 4626−4630.
(36) Griffiths, P. R.; de Haseth, J. A. *Fourier Transform Infrared Spectrometry*; John Wiley & Sons, Inc.: Hoboken, NJ, 2007.